Molecular and Cellular Pathobiology

Transcriptional Pathway Signatures Predict MEK Addiction and Response to Selumetinib (AZD6244)

Jonathan R. Dry[1], Sandra Pavey[4], Christine A. Pratilas[5], Chris Harbron[2], Sarah Runswick[1], Darren Hodgson[3], Christine Chresta[1], Rose McCormack[2], Natalie Byrne[1], Mark Cockerill[1], Alexander Graham[1], Garry Beran[1], Andrew Cassidy[1], Carolyn Haggerty[1], Helen Brown[1], Gillian Ellison[2], Judy Dering[6], Barry S. Taylor[5], Mitchell Stark[4], Vanessa Bonazzi[4], Sugandha Ravishankar[4], Leisl Packer[4], Feng Xing[5], David B. Solit[5], Richard S. Finn[6], Neal Rosen[5], Nicholas K. Hayward[4], Tim French[1], and Paul D. Smith[1]

Abstract

Selumetinib (AZD6244, ARRY-142886) is a selective, non–ATP-competitive inhibitor of mitogen-activated protein/extracellular signal–regulated kinase kinase (MEK)-1/2. The range of antitumor activity seen preclinically and in patients highlights the importance of identifying determinants of response to this drug. In large tumor cell panels of diverse lineage, we show that MEK inhibitor response does not have an absolute correlation with mutational or phospho-protein markers of BRAF/MEK, RAS, or phosphoinositide 3-kinase (PI3K) activity. We aimed to enhance predictivity by measuring pathway output through coregulated gene networks displaying differential mRNA expression exclusive to resistant cell subsets and correlated to mutational or dynamic pathway activity. We discovered an 18-gene signature enabling measurement of MEK functional output independent of tumor genotype. Where the MEK pathway is activated but the cells remain resistant to selumetinib, we identified a 13-gene signature that implicates the existence of compensatory signaling from RAS effectors other than PI3K. The ability of these signatures to stratify samples according to functional activation of MEK and/or selumetinib sensitivity was shown in multiple independent melanoma, colon, breast, and lung tumor cell lines and in xenograft models. Furthermore, we were able to measure these signatures in fixed archival melanoma tumor samples using a single RT-qPCR–based test and found intergene correlations and associations with genetic markers of pathway activity to be preserved. These signatures offer useful tools for the study of MEK biology and clinical application of MEK inhibitors, and the novel approaches taken may benefit other targeted therapies. *Cancer Res; 70(6); 2264–73. ©2010 AACR.*

Introduction

Selumetinib (AZD6244, ARRY-142886) is a potent, orally active inhibitor of mitogen-activated protein/extracellular signal–regulated kinase (ERK) kinase (MEK)-1/2 (1) that suppresses the pleiotropic output of the RAF/MEK/ERK path-

Authors' Affiliations: [1]Cancer Bioscience, [2]DECS, and [3]Clinical Biomarker Group, AstraZeneca R&D, Alderley Park, Macclesfield, United Kingdom; [4]Oncogenomics Laboratory, Queensland Institute of Medical Research, Herston, Australia; [5]Departments of Medicine, Pediatrics, Computational Biology, and Molecular Pharmacology and Chemistry, and the Human Oncology and Pathogenesis Program, Memorial Sloan-Kettering Cancer Center, New York, New York; and [6]Oncology Geffen School of Medicine, Division of Hematology, Department of Medicine, University of California, Los Angeles, Los Angeles, California

Corresponding Author: Jonathan R. Dry, 33G83 Mereside, Alderley Park, Macclesfield, Cheshire SK10 4TG, United Kingdom. Phone: 44-625-233699; Fax: 44-625-510097; E-mail: Jonathan.Dry@astrazeneca.com.

©2010 American Association for Cancer Research.

way (Supplementary Fig. S1) and thus has potential to block cell proliferation, survival, and/or invasion depending on cell type. Pathway-activating mutations in BRAF (2) are prevalent in a number of tumor types (Supplementary Fig. S1) and have been linked to cell line sensitivity to MEK inhibition (3), raising the prospect that pharmacologic inhibition of this pathway could have clinical benefit (4, 5) in selected patients. Mutant Ras has also been linked to sensitivity to MEK inhibition (1, 5); however, this link is complex because RAF represents only one of several Ras effector pathways, including phosphoinositide 3-kinase (PI3K), that may offer a compensatory route to cell proliferation/survival (refs. 6, 7; Supplementary Fig. S1).

Diagnostics that successfully guide clinical treatment decisions (8) include the measurement of Her2 status for trastuzumab treatment of breast cancer and *KRAS* mutation for colorectal cancer resistance to cetuximab (9, 10). Measurement of individual markers, however, is unlikely to capture the inherent biological complexity of growth factor signaling pathway dependence (11). Multivariate approaches such as microarrays have the potential to assess functional activation of the drug target alongside "compensatory signaling," yet the dimensionality of microarray data demands large sample numbers to support robust biomarker discovery (12). The utility of this technology has been shown for established therapeutics in early

American Association for Cancer Research

breast cancer, where access to large clinical data sets has led to the development of Mammaprint and OncotypeDX (9, 13, 14), which have received approval from the Food and Drug Administration and been included in early clinical guidelines, respectively. For drugs in early development, however, relatively few patients are treated, forcing a reliance on preclinical models such as tumor cell lines for hypothesis generation.

Recent studies have illustrated the potential for gene signatures derived from preclinical platforms to be predictive of clinical drug response (15–17); however, the genes prioritized within such signatures can vary widely as a result of small differences in the statistical or experimental approaches taken (18). As an example, a nonredundant set of all genes in 15 published signatures predictive of RAS/RAF/MEK/ERK activity (Supplementary Document S1) comprises >16,000 genes. Few (<1%) of these genes are consistently represented in multiple signatures, highlighting the high false-positive rate and therefore limited potential for cross-predictivity from any one of these signatures alone. These observations suggest that a combination of large cell line panels and enhanced approaches to select biologically and statistically robust gene sets is essential if a clinically relevant signature is to be generated preclinically (19).

Using large cell panels of diverse tumor types, we took a novel approach to discover candidate gene expression signatures predictive of functional output from pathways relating to selumetinib response. Two key signatures were identified. The first (18 genes) provides a measure of MEK functional output independent of the mutational status of BRAF/RAS, whereas the second (13 genes) predicts drug resistance in the presence of active MEK independently of PI3K mutation. The signatures predict baseline and dynamic pathway activity and sensitivity to selumetinib in independent cell line panels and xenografts. Furthermore, these signatures were robustly measurable in fixed human tumor samples, where correlative expression relationships were preserved between genes within signatures and between signatures and pathway mutational markers.

Materials and Methods

Cell culture and cell viability assays. Two data sets from mixed-tumor (1)[7] and melanoma (20) cell line panels were used to identify biomarkers of selumetinib. Further testing was run in independent colon (21) and breast (22) cell panels. Cells were cultured in RPMI 1640 supplemented with 10% fetal bovine serum. *In vitro* GI_{50} is the concentration of selumetinib required to control cell growth by 50% in a 72-h period, as determined by the colorimetric 3-(4,5-dimethylthiazol-2-yl)-5-(3-carboxymethoxyphenyl)-2-(4-sulfophenyl)-2*H*-tetrazolium assay (ref. 1; Supplementary Table S1).

An additional mixed-tumor cell panel (23) was exposed to PD0325901 or DMSO control for 8 h as previously described (ref. 24; Supplementary Table S2).

Genetic profiling of cell lines. Genetic screening in the melanoma (20, 25), breast (22), and drug-treated (23, 24) cell

panels has been described previously. For other cells, genomic DNA was extracted using the Puregene method (Gentra Systems). Primers were designed around each of the exons of interest to include *BRAF* (exon 15), *KRAS* (exons 2 and 3), *HRAS* (exons 2 and 3), *NRAS* (exons 2 and 3), and the entire coding sequences of *PTEN, AKT1, AKT2*, and *AKT3*. For each sample, 25 ng of genomic DNA were amplified with an MJ tetrad thermal cycler. The PCR products were sequenced using BigDye terminator cycle sequencing kit (v3.1, Applied Biosystems) on a 3730 DNA Analyzer (Applied Biosystems). Cell line genomic amplification/deletion was measured by comparative genomic hybridization using Agilent 244K DNA microarrays following the manufacturer's standard protocols[8] (z score threshold of 3.0).

Western blot analysis of cell lines. Cells in log-phase growth were harvested and frozen at –80°C; cell pellets were lysed from frozen in buffer containing DNase, protease, and phosphatase inhibitors. Protein was quantified using bicinchoninic acid (Pierce), resolved by SDS-PAGE, and transferred onto nitrocellulose membranes (Invitrogen). Histone H3 displayed minimal variability in expression between cell types and was selected as a loading control.

Oligonucleotide expression array analysis of cell lines. For each cell line in the melanoma, mixed-tumor, colon, and drug-treated panels, 4 μg of total RNA were isolated (RNeasy Mini Kit, Qiagen[9]) and gene expression was measured using Affymetrix HG U133 Plus 2.0 GeneChip arrays following standard protocol[10,11] and as previously described (20, 23). Affymetrix gene expression was quantified by robust multiarray analysis, and data collapsed gene centrically (EntrezID) following probe-set QC (Supplementary Tables S2 and S3). For the breast cell panel, expression was measured as the log ratio between individual cell lines and a breast cell line mixed reference pool using the Agilent Human 1A V1 chip as previously described (22).

Gene expression data analysis. The approaches taken to identify and independently test gene expression signatures are summarized in Fig. 1, with further detail available in Supplementary Fig. S2.

"Transcriptome networks" predictive of pathway activity were defined as groups of genes displaying the following characteristics:

1. Differential expression in a subset of exclusively resistant or sensitive cell lines (Supplementary Fig. S3A). For each gene, a high-expressing and a low-expressing subset of cell lines were identified by *k*-means clustering with $k = 2$ and/or measurement of bimodal/nonnormal distribution. Genes were prioritized where one of these subsets was exclusively populated by cell lines of the same drug sensitivity. Results were compared with

---

[7] http://www.atcc.org

[8] http://www.agilent.com
[9] http://www.qiagen.com/
[10] http://www.mged.org/Workgroups/MIAME/miame.html
[11] http://www.affymetrix.com/support/technical/manual/expressionmanual.affx

ANOVA, two-dimensional false discovery rate, and regression analysis of log GI_{50}.

2. Networks of intercorrelated expression (ref. 17; Supplementary Fig. S3B). Networks of coexpressed genes were defined as those displaying a Pearson correlation approaching that typically observed between redundant probe sets for a given gene. Genes within such networks were prioritized where gene-gene correlations were reproducible across independent data sets or supported (with consistent directionality) by published biological interactions [entity relationships (KEGG[12]; Ingenuity Pathways Analysis, Ingenuity Systems[13]), interaction-based co-occurrence in Medline articles (Linguamatics I2E[14] and Quosa[15]), or colocalization in the genome].

3. Dynamic gene expression reflective of pathway activity. From literature[16] and online databases (GEO[17], Oncomine; ref. 26), we were able to identify 109 "transcriptome" signatures reflecting inhibition or activation of targets in several oncogenic pathways (aDOPT database, Supplementary Document S1). Genes consistently differentially expressed in multiple signatures for a common pathway were prioritized.

Potential mRNA markers of selumetinib response were ranked relative to the quantity, quality, and consistency of supporting statistical and biological annotation. One hundred eighty-one genes, representing the number expected to be measurable by RT-qPCR in clinical tissue, were prioritized for further validation. An aggregate measure of the gene expression from each transcriptome network was calculated by scaling probe-set expression values between 0 (min across all cell panels) and 1 (max), taking the mean gene centrically and then taking the mean for genes within a network.

Biomarker measurement in formalin-fixed paraffin-embedded melanoma samples. Commercially available formalin-fixed paraffin-embedded (FFPE) melanoma tumor sections were sourced from Asterand and subjected to histopathologic assessment of tumor content. DNA was extracted as previously described (27) and *BRAF* mutation measured using ARMS (Supplementary Table S4). RNA was isolated using an optimized FFPE RNA system (Ambion), RNA was quantified (NanoDrop).

RT-qPCR confirmation of gene expression. Expression profiles were validated in the cell lines and FFPE melanoma tissue samples by one-step RT-qPCR on 100 ng of total RNA (Quantitect, Qiagen[10]) and 100 μL of PCR mix per sample using ABI 7900HT on customized TaqMan low-density arrays (TLDAs; Applied Biosystems). Gene expression profiling

was done on four arrays (48 format P/N 4346800), each including 45 target genes and 3 normalization genes. The normalization genes were 18S rRNA (manufacturer's mandatory housekeeping gene), *PGK1*, and *PSMB2*. These were selected from a panel of housekeeping genes as they showed minimal variability in expression across the cell lines and melanoma FFPE samples. Expression data were normalized to the average ΔCt for *PGK1* and *PSMB2*.

Results

Cell lines and response to MEK inhibition. Cell lines were classified as sensitive (<1 μmol/L) or resistant (>10 μmol/L) based on the GI_{50} distribution profile (Fig. 2) and predictions for the clinically achievable concentration of drug. This left a 10-fold "intermediate" window to allow for variability in the cell profiling data. The cell line sensitivity profile of selumetinib did not correlate with agents targeting unrelated pathways, highlighting the determinants of response to be mechanistic and not prognostic.
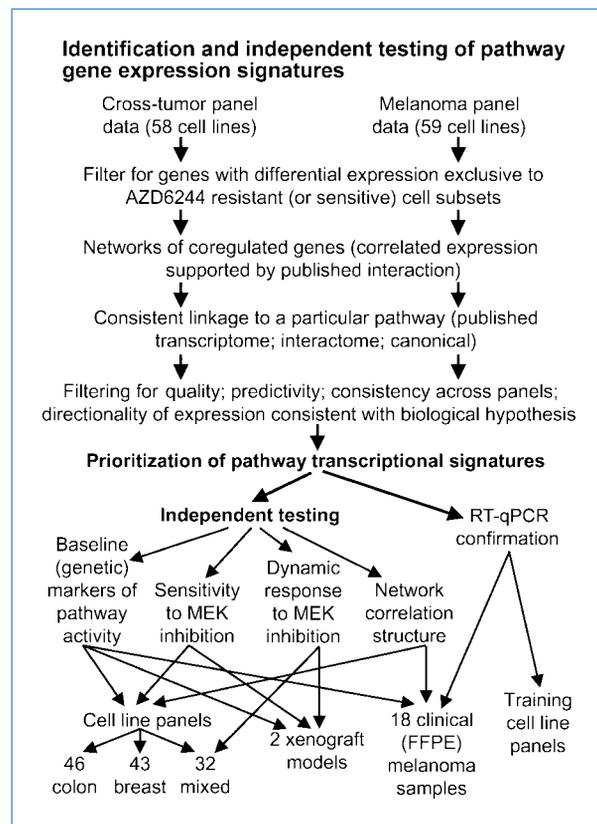
Figure 1. Preprocessing and gene expression analysis were done separately for each of the mixed-tumor and melanoma cell line panels. Transcriptional signature gene expression was tested against selumetinib (AZD6244) sensitivity and dynamic pathway activity in multiple independent data sets. Methods were partially automated using R (http://www.r-project.org/) and workflow technology (InforSense KDE, http://www.inforsense.com/). RT-qPCR, reverse transcription quantitative PCR.

[12] http://www.genome.jp/kegg/pathway.html
[13] http://www.ingenuity.com
[14] http://www.linguamatics.com/
[15] http://www.quosa.com/
[16] http://www.ncbi.nlm.nih.gov/pubmed/
[17] http://www.ncbi.nlm.nih.gov/geo/

Figure 2. A consistent bimodal distribution of cell lines is seen relative to selumetinib GI_{50} in both the mixed-tumor (A) and melanoma (B) panels, suggesting distinct populations of responding (<1 μmol/L) and resistant (>10 μmol/L) cell lines. In the mixed-tumor panel, *BRAF* and, to a lesser extent, *RAS* mutations are concentrated in sensitive cell lines, whereas a trend is visible for mutational activation of the PI3K pathway (deletion/amplification/point mutation in *PTEN, PI3K,* or *AKT*) in resistant cell lines. Responding cell lines and differing genetic phenotypes are unevenly distributed across cells of differing tissues of origin (controlled for within statistical analyses).
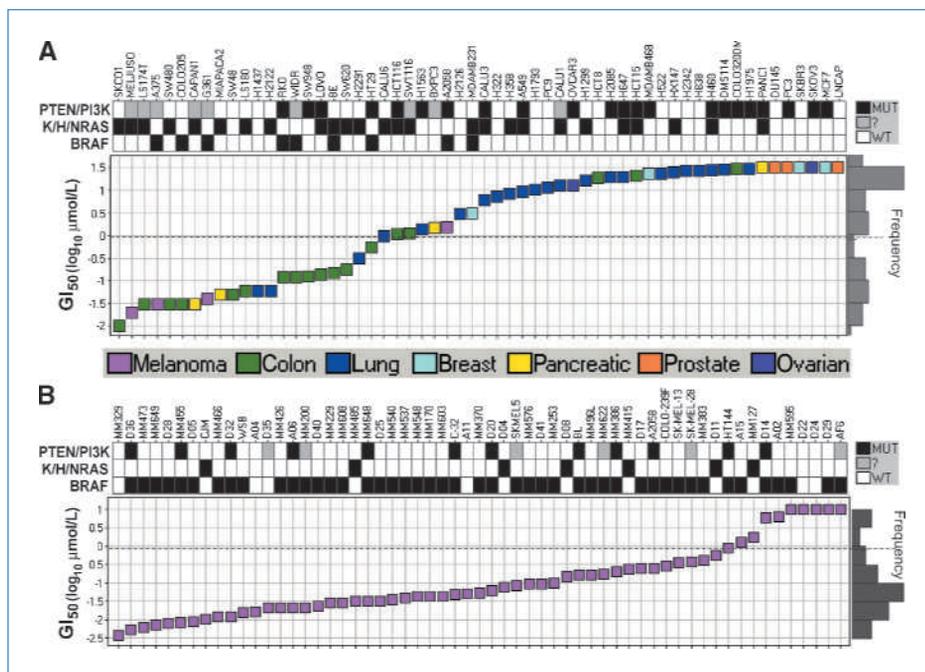
Hypothesis testing of previously identified candidate markers. Higher frequency of *BRAF* mutation was seen in melanoma and colorectal cell lines (Fig. 2), and *RAS* mutation was more prominent in colorectal and lung, agreeing with the clinical distribution represented in the COSMIC database[18] (Supplementary Fig. S1). A significant relationship between cell line sensitivity to selumetinib and *BRAF* or *KRAS* mutation was seen in the mixed-tumor panel (Fig. 2A; Supplementary Fig. S4). Prediction was enhanced by combining these two oncogenes ($P < 0.0001$, sensitivity = 0.86, specificity = 0.76; Supplementary Fig. S5) and further still by accounting for resistance measured through genetic loss of *PTEN* function or activation of PI3K/Akt (Fig. 2; Supplementary Fig. S5). No relationship between sensitivity and *BRAF/RAS* mutation was observed in the melanoma panel (Fig. 2B); however, the number of resistant and wild-type (WT) *BRAF* cell lines was limited. Although a trend is visible for elevated phospho-total ERK protein and reduced phospho-Akt in sensitive cell lines (Fig. 3), the relationship is not absolute and no significant prediction of response was achieved from quantified values (Supplementary Fig. S6).

Generation of novel candidate multivariate markers of pathway activity and selumetinib response. We hypothesized that genes reflective of activity and functional output from the drug target, MEK, would have the following characteristics: low expression exclusive to a consistent subset of resistant cell lines (e.g., Supplementary Fig. S3); reproducibility in independent data sets; and overlap with signatures of

dynamic activity of RAS, RAF, MEK, and/or ERK. Eighteen correlated genes showed this combined profile and were termed a "MEK-functional-activation" network/signature (Fig. 4A and B; Supplementary Fig. S7). Cell lines harboring MEK pathway–activating mutations typically showed high baseline expression of genes in this signature (Fig. 4C and D; Supplementary Fig. S8A).

By extension, we also hypothesized that genes reflective of core resistance mechanisms would show consistently high expression in one or more subsets of resistant cell lines. We identified a 13-gene "compensatory-resistance" network/signature overlapping dynamic signatures of RAS/MAPK activity, but importantly not RAF/MEK/ERK (Fig. 4A and B; Supplementary Fig. S7). Expression from this signature did not correlate to RAS or PI3K pathway mutations, was typically low in cells with *BRAF* mutation, and was never seen without expression of MEK-functional-activation (Fig. 4C and D; Supplementary Fig. S8B). These observations highlight a potential role in resistance for compensatory signaling through RAS effectors other than RAF-MEK or PI3K that are attenuated where MEK dependence is highest.

By plotting the aggregate gene expression measurement for MEK-functional-activation against compensatory-resistance, we were able to separate drug-sensitive from drug-resistant cell lines (Fig. 5A). This predictivity was reproducible in both the melanoma and the mixed-tumor panels irrespective of tissue of origin, panel, or mutation status, with optimal sensitivity of 0.96 and specificity of 0.82.

Collectively, these data suggest that where MEK activation originates upstream of RAF, the preference of signaling from RAS is the primary determinant of response to selumetinib. The complexity of resistance, however, is further illustrated

---

[18] http://www.sanger.ac.uk/genetics/CGP/cosmic/
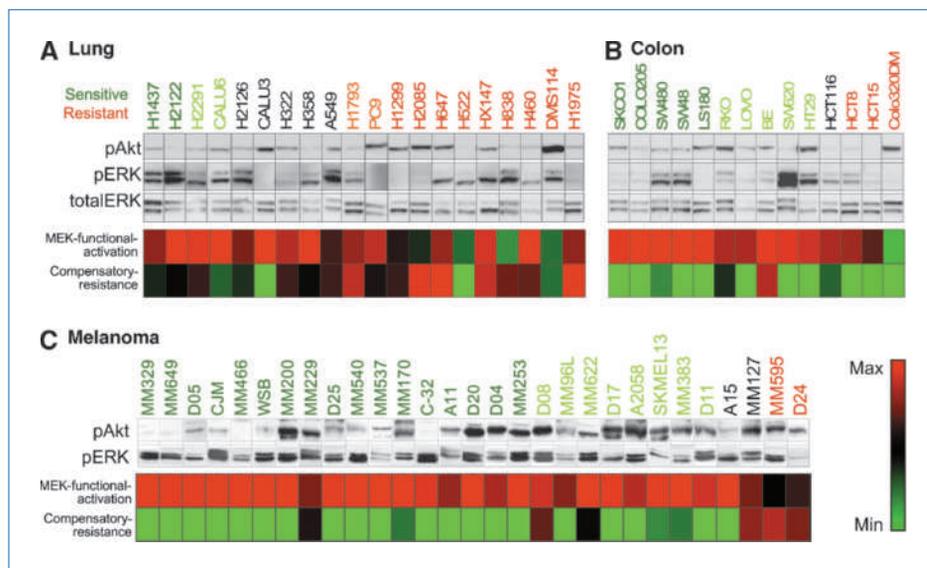
Figure 3. Western blots of lung (A), colon (mixed-tumor panel; B), and melanoma (C) cell lines, ordered by response (GI$_{50}$) to selumetinib, suggest a range of pERK and pAkt expression in both sensitive and resistant cells. In resistant cell lines, trends are visible for low pERK (suggesting inactivity of MEK), or high pERK alongside high pAkt (suggesting that dependency on MEK signaling is reduced through PI3K activity); however, these relationships are not absolute. Scaled mean expressions from mRNA signatures identified as predictive of selumetinib response are also shown, with little correlation obvious between pERK and MEK-functional-activation or between pAkt and compensatory-resistance.

by the identification of other smaller gene networks associating alternative mechanisms with resistance (Supplementary Fig. S9), described in Supplementary Table S5. In total, 181 genes were prioritized as potential markers of response, 67 of which displayed consistent expression trends in both the cross-tumor and melanoma cell panels (Supplementary Table S5). That the gene selection approaches taken afforded enhanced reproducibility is perhaps best illustrated by comparison to gene sets identified by filtering on P value from the t test statistical method that, in contrast to those described in this article, show little crossover between cell panels (Supplementary Table S6). The limited representation of canonical pathway components in our signatures, and the resulting reliance on literature-derived pathway transcriptome signatures, is also noteworthy (Fig. 4A; Supplementary Table S7).

Performance of signatures in independent* in vitro, in vivo*, and clinical data sets. The power of the MEK-functional-activation and compensatory-resistance gene expression signatures to predict selumetinib response was reproducible at the same threshold in an independent panel of 46 colorectal cell lines (Fig. 5B), with a sensitivity of 1 and a specificity of 1. Notably, despite the low representation of breast cell lines in the mixed-tumor panel, a high level of predictivity was also achieved across a panel of 43 breast cell lines (ref. 22; Fig. 5C) using an independent gene expression platform, with an optimal sensitivity of 0.78 and a specificity of 0.96. Consistent trends were also seen for high MEK-functional-activation expression in cells known to be enriched for MEK signaling and for low compensatory-resistance where MEK-functional-activation was low (Figs. 5 and 6; Supplementary Fig. S10; refs. 6, 22).

Using data from the Gene Expression Omnibus (GSE3542), we showed that the MEK-functional-activation signature was elevated following transfection of activated MEK into estrogen receptor–positive breast cancer cells (Fig. 6A;

ref. 28). In addition, this signature showed consistently reduced expression in 32 cell lines treated with a different MEK inhibitor, PD0325901 (Fig. 6B). As expected, cell lines sensitive to MEK inhibition tended to harbor MEK-activating mutations in *BRAF* or *RAS* and displayed a higher baseline MEK-functional-activation expression that was dramatically reduced following MEK inhibition. BRAF^{V600E} lines known to harbor PI3K pathway–activating mutations also followed this pattern of MEK-functional-activation expression, but showed varying sensitivity consistent with trends seen in other cell panels (Fig. 6B). Lower MEK dependency in receptor tyrosine kinase (RTK)–driven cell lines was indicated by low baseline expression from the MEK-functional-activation signature, predictive of resistance to inhibition and supporting previously published observations (24). We were also able to confirm this genotype-specific reduction in MEK-functional-activation expression following MEK inhibition in tumor xenograft models (Fig. 6C; ref. 24).

A key objective of this work was to measure these transcriptome networks in clinical tissue. When confirmed by RT-qPCR, expression of each gene showed a Pearson correlation of >0.6 to Affymetrix data across the mixed-tumor and melanoma cell panels (e.g., DUSP6; Supplementary Fig. S11). In 18 FFPE early-stage melanoma patient samples, all genes were detectable in at least 90% of the tissue samples when measured by the same approach. Wilcoxon tests showed a statistically significant enrichment (P = 0.033) of higher intergene correlations across tissue samples for genes within the MEK-functional-activation and compensatory-resistance transcriptome network signatures, confirming that the correlations translate into similar relationships within melanoma tissue. Notably, the MEK-functional-activation signature showed a higher correlation to *BRAF* mutation status across the melanoma tissue samples than the other genes measured, and also low expression was only seen in *BRAF* WT samples (Fig. 6D).

Discussion

Exploration of the MEK/ERK signaling pathway has revealed significant complexity to be considered when modeling response to MEK inhibitors. Functional activation of MEK can be driven from RAF, RAS, or RTKs, and resistance can be mediated by different compensatory mechanisms including alternative RAS/RTK effectors such as PI3K (Fig. 1A). This level of pathway interplay highlights the challenge of identifying biomarkers to predict dependence on MEK.

Previous studies have linked BRAF and, more weakly, RAS mutations to *in vitro* sensitivity to MEK inhibition (1, 3, 5, 7)

and PI3K pathway–activating mutations to resistance (6, 7). The results from the present study using selumetinib support this general observation, but reveal these relationships to be far from absolute when assessed across a larger, more diverse collection of cell types (Fig. 2). A similar trend was observed for protein markers of MEK/ERK and PI3K pathway activation, with pERK and pAkt proving to be less robust markers of pathway output than previously suggested (refs. 5, 7, 24; Fig. 3). It is perhaps not surprising that individual mutation or protein measurements fail to adequately predict pathway activity considering the complexity of signal control through the MEK/ERK axis. To provide a more
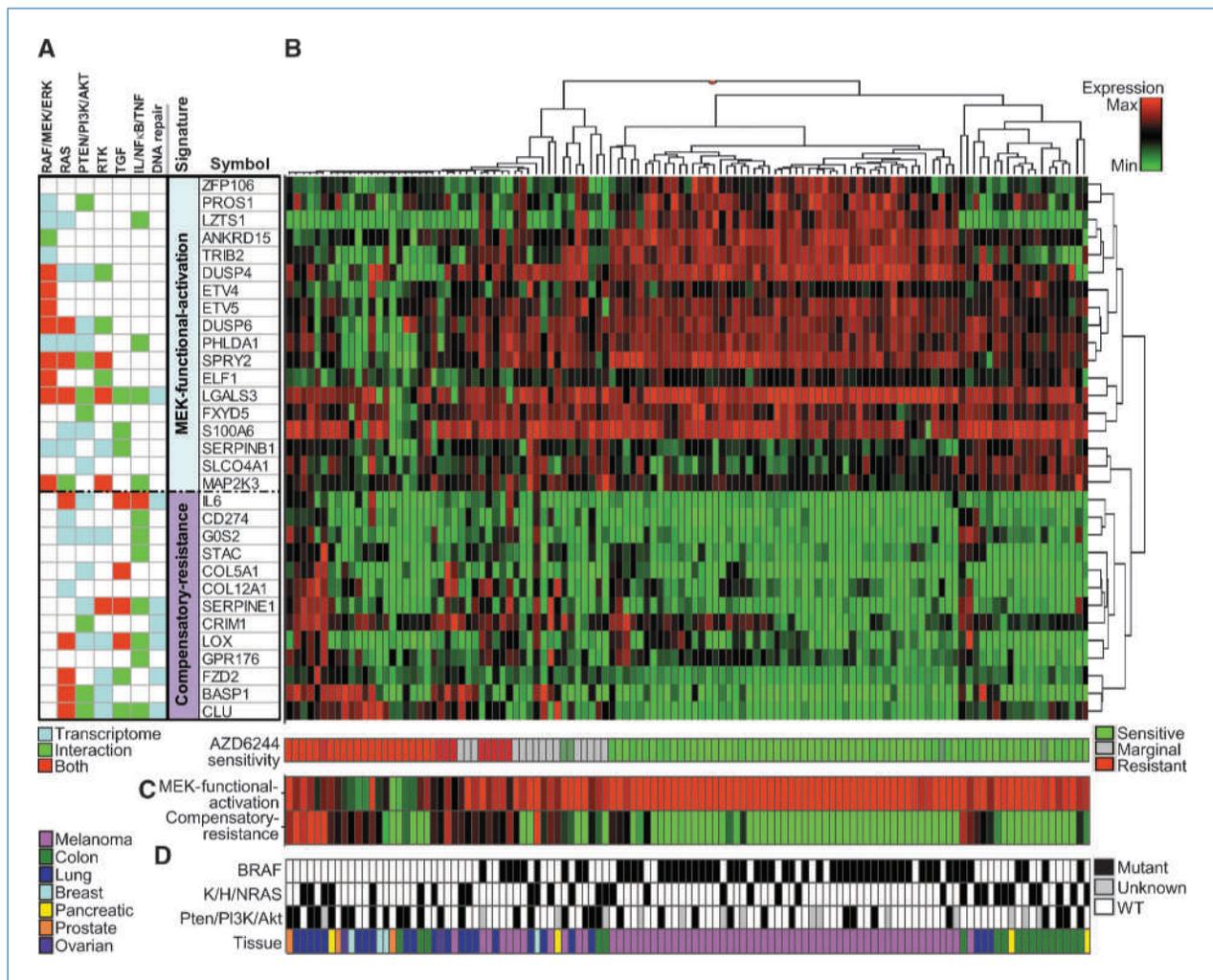
Figure 4. A, genes prioritized in the MEK-functional-activation and compensatory-resistance network signatures are shown. The identification of genes displaying consistent expression in published pathway transcriptome signatures enhanced biological characterization otherwise achieved through protein interaction/canonical pathway based information. RAF/MEK/ERK biological overlay is seen exclusively in the MEK-functional-activation signature, whereas RAS signaling alongside that linked to broader MAPK activity (PTEN/PI3K, TGF/TNF/IL-6/NF-κB and DNA repair; refs. 7, 24, 38, 39) is concentrated to the compensatory-resistance signature genes. B, unsupervised clustering highlights correlations between genes within transcriptome network signatures and separates selumetinib (AZD6244) responsive from nonresponsive cell lines. C, taking the mean scaled expression for genes within signatures highlights the cell line subset–specific nature of expression, with MEK-functional-activation exclusively low in a resistant cell line subset and high compensatory-resistance limited to a subset of resistant cell lines. D, cell lines harboring BRAF and, to a lesser extent, RAS activating mutations display high expression of the MEK-functional-activation signature. No obvious correlation is visible between compensatory-resistance signature expression and RAS and/or PI3K pathway mutations.
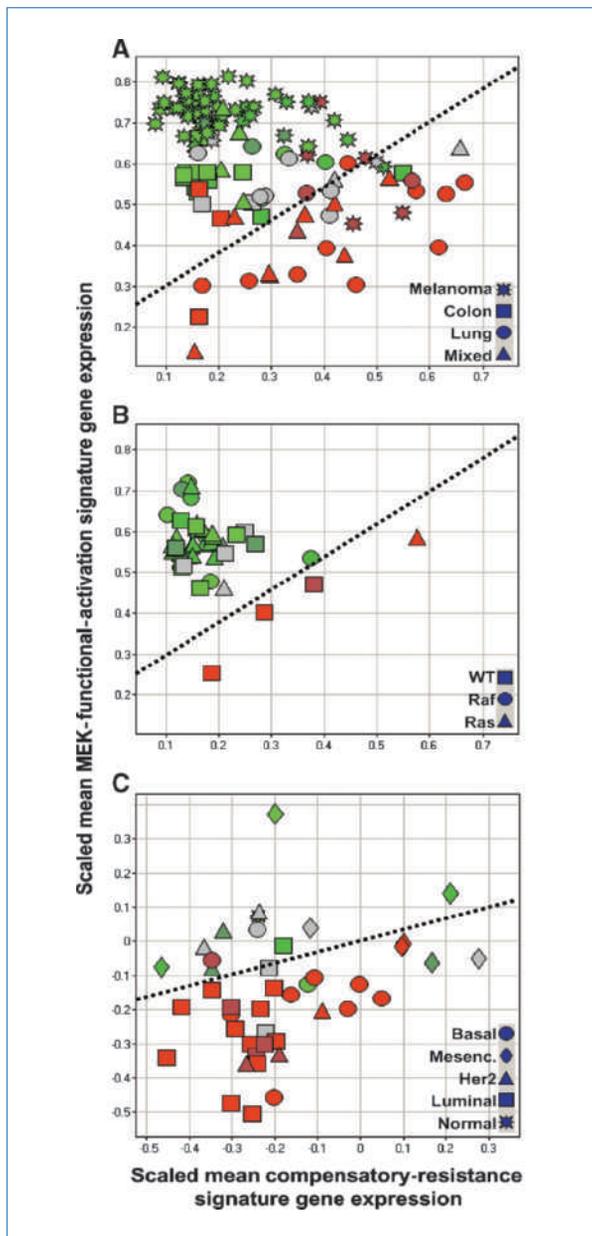
Figure 5. Selumetinib sensitive (green) cell lines show higher MEK-functional-activation and/or lower compensatory-resistance signature expression. The converse is true of resistant (red) cell lines, and cells of intermediate sensitivity (gray) lie in between. In no cases is high compensatory-resistance expression seen without expression of MEK-functional-activation, suggesting that the mechanisms represented by these signatures are not mutually exclusive. A, the threshold at which optimal separation of sensitive from resistant cell lines is achieved in the mixed-tumor/melanoma cell panels is illustrated with a dotted line. B, consistent separation at the same threshold is achieved in an independent panel of colon cell lines, where all BRAF-mutant tumors show high expression of the MEK-functional-activation signature. C, signatures also show a consistent trend relative to response in an independent breast cell panel, where higher MEK-functional-activation expression is predominantly seen in the basal/mesenchymal subtype known to show higher activity of MEK (6). As expression in this breast panel was measured using a different gene expression platform, threshold values are not directly comparable to those in A and B.

comprehensive molecular assessment of pathway status, we set out to identify gene expression networks that more accurately predict sensitivity to MEK inhibition. Furthermore, we used large cell panels to at least partially reflect known heterogeneity in tumor biology and increase the likelihood that *in vitro* signatures can be translated into the clinical setting.

By incorporating biological assumptions within the statistical approach taken (Fig. 1; Supplementary Fig. S2), we prioritized two gene transcription networks as markers of functional output from pathways that act cooperatively to predict response to selumetinib *in vitro*. This predictivity was reproducible across independent cell panels of diverse tumor origin, even when profiled in different laboratories using alternative technology platforms (Fig. 5). The largest of these networks comprised 18 genes capturing transcriptional events common to MEK/ERK functional output and has therefore been termed the MEK-functional-activation signature (Fig. 4A; Supplementary Fig. S7a). This signature contains dual-specificity phosphatases (DUSP4/6; refs. 24, 29), sprouty homologue 2 (SPRY2; refs. 24, 30), and pleckstrin homology-like domain family A member 1 (PHLDA1; ref. 31), all of which are known transcriptional targets of MEK/ERK signaling involved in negative feedback regulation of ERK and its upstream modulators. Other known transcriptional targets of MEK/ERK signaling present in the signature are the Ets variant transcription factors (ETV4, ETV5, and ELF1; refs. 32, 33), alongside other MEK family members (MAP2K3) potentially coactivated by signals activating MEK1/2. The signature also suggests the importance of other genes previously linked to regulation of MAPK signaling, cell cycle, and tumor prognosis, including tribbles 2 (TRIB2; ref. 34), galectin 3 (LGALS3; ref. 35), and the transcription factors KANK1 (ANKRD15) and leucine zipper (LZ-) TS1 (36, 37).

Whereas *BRAF/RAS* mutation (Fig. 2) and pERK protein measurements (Fig. 3) vary across cells that respond to selumetinib, expression of the MEK-functional-activation signature is consistently high (Figs. 4–6; Supplementary Fig. S10). Furthermore, expression of this signature is dynamically increased following MEK activation (28) and decreased following MEK inhibition in multiple tumor cell lines and xenografts (ref. 24; Fig. 6A–C). Collectively, these data show the biologically relevant and robust measurement of MEK pathway output and inhibition given by this signature, independent of the pathway activation point, highlighting its utility as both a predictor of drug sensitivity and a marker of pharmacodynamic response. Because the MEK pathway can be functional in cells that display resistance to MEK inhibition, this signature may also enable a more rational selection of preclinical models (and perhaps patients) in which to test drug combinations (Supplementary Fig. S12), especially if the nature of the compensatory pathways that mask MEK dependence can be identified.

The second network identified was reproducibly predictive of resistance in cells with MEK functional activity across independent cell panels and was termed compensatory-resistance (Fig. 4A). Biological overlay suggested that this signal may be the result of a branch in signaling upstream of RAF/MEK,
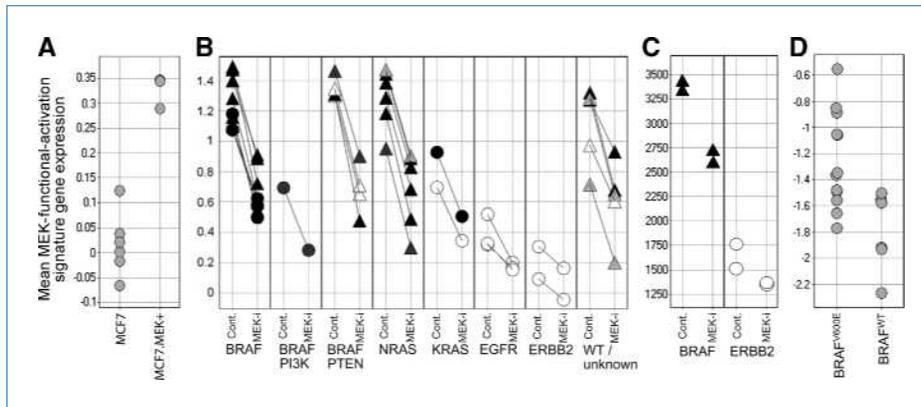
Figure 6. A, the MEK-functional-activation signature is significantly upregulated following transfection of activated MEK into the MCF7 cell line (28). B, furthermore, a knockdown of MEK-functional-activation signature expression is consistently seen following MEK inhibition with PD0325901 across cell lines (pairs joined with a solid line) independent of tissue of origin (triangle, melanoma; circle, other). Cells responsive to MEK inhibition (black to gray) show higher MEK-functional-activation expression in the DMSO-treated control and typically harbor mutations in *BRAF* or *NRAS*. RTK (EGFR/ERBB2)-driven cell lines show markedly lower starting MEK-functional-activation expression and are predominantly resistant to MEK inhibition (white). BRAF[V600E] PTEN-mutant cells show higher MEK-functional-activation expression but variable sensitivity to MEK inhibition. C, this genotype-specific pattern of MEK-functional-activation expression is reproducible in BRAF-activated (SKMEL28) and ERBB2-amplified (BT474) tumor xenograft models following MEK inhibitor treatment (24). D, although expression from the MEK-functional-activation signature seems to be high in most FFPE melanoma tissue samples, there is a trend for highest expression from patients harboring mutations in *BRAF*, with lower expression limited to *BRAF* WT.

with consistent transcriptional regulation by RAS seen for the majority of these genes (Fig. 4A, Document S1). This hypothesis was supported as expression of the compensatory-resistance signature was low in BRAF-mutant cells (Fig. 4; Supplementary Fig. S9B) and was not seen without MEK activity (Fig. 5). The signature comprises a diverse set of genes with common linkage to transforming growth factor-β (TGF-β)/tumor necrosis factor-α (TNF-α)/NF-κB signaling (Fig. 4A; Supplementary Fig. S7B; refs. 38, 39). A number of these genes are known to regulate signaling pathways that offer an alternative route to cell proliferation, for example, activation of the G-protein–coupled receptor frizzled homolog 2 (FZD2), which activates WNT signaling (40), or activation of Jak-STAT by interleukin-6 (IL-6; ref. 41). Alongside these are a number of genes potentially offering enhanced cell survival and chemoresistance through control of tumorigenic processes such as hypoxia/angiogenesis (serine protease SERPINE1, lysyl oxidase LOX, and collagens COL5A1 and COL12A1), cell cycle [G_0/G_1 switch 2 (GOS2)], proliferation/apoptisis [cysteine-rich transmembrane BMP regulator 1 (CRIM1; ref. 42) and clusterin (CLU; ref. 43)], and immune evasion (CD274; ref. 44).

The implication that, where MEK is active, Ras effector signaling through PI3K may mediate resistance to MEK inhibition is not new (6, 7, 23, 45, 46). Surprisingly, however, expression of the compensatory-resistance signature seemed to be independent of PI3K pathway activation (Fig. 4; Supplementary Fig. S8B), contradicting the literature precedent that PI3K activity alone may be the primary determinant of resistance (6, 7, 23, 46). Where MEK activity is driven from a point upstream of RAF, expression from this compensatory-resistance signature potentially enables better separation of cells with lower MEK dependence.

Having assembled these transcript networks and shown their *in vitro* predictive power and ability to recapitulate

known biology, we sought to assess their potential as biomarkers in the clinical setting. We showed that the MEK-functional-activation and compensatory-resistance signatures can be reliably detected in fixed clinical tissue using a single RT-qPCR–based test and that the internal correlation structure of these gene networks is preserved. Furthermore, we showed the expression of the MEK-functional-activation signature to be higher in BRAF-mutant than in WT melanoma (Fig. 6D), indicating that detectable transcriptional wiring is comparable between preclinical and clinical samples. From these data, we believe that it is feasible to use a single test measuring mRNA signatures as an investigative predictive biomarker in clinical trials for MEK-targeted therapies. A key challenge in this context will be the translation of gene expression thresholds set by preclinical data to give clinically relevant patient selection. It is likely that a training step will be necessary to first optimize the aggregation and application of gene signatures to suit the tissue type being measured (Fig. 6) and the gene expression platform being used (Fig. 5). Considerations also need to be taken when designing broader application of such a test in the clinic, with standardized operating procedures necessary to control for the confounding effects of variables such as differing protocols, age of samples, and fixation methods (47).

In summary, the methods outlined in this article aim to improve the biological and clinical relevance of hypotheses generated from preclinical gene expression data. We identified transcript signatures, robustly detectable using a single test in fixed clinical tissue, enabling enhanced measurement of baseline/dynamic functional activity from MEK and prediction of response to selumetinib. These signatures can identify MEK dependency irrespective of the genetic or cell-specific factors that determine signaling

preferences, particularly in cells where MEK is only one output of a more pleiotropic upstream signal (e.g., RAS mutation). Although we have focused on identifying transcriptome signatures related to response to MEK inhibition, the approach is equally applicable if extended to other drug targets and signaling pathways, particularly where genetic markers of response are unknown or insufficient to capture complex signaling.

Disclosure of Potential Conflicts of Interest

No potential conflicts of interest were disclosed.

References

1. Davies BR, Logie A, McKay JS, et al. AZD6244 (ARRY-142886), a potent inhibitor of mitogen-activated protein kinase/extracellular signal-regulated kinase kinase 1/2 kinases: mechanism of action *in vivo*, pharmacokinetic/pharmacodynamic relationship, and potential for combination in preclinical models. Mol Cancer Ther 2007;6:2209–19.
2. Brose MS, Volpe P, Feldman M, et al. BRAF and RAS mutations in human lung cancer and melanoma. Cancer Res 2002;62:6997–7000.
3. Solit DB, Garraway LA, Pratilas CA, et al. BRAF mutation predicts sensitivity to MEK inhibition. Nature 2006;439:358–62.
4. Sebolt-Leopold JS, Dudley DT, Herrera R, et al. Blockade of the MAP kinase pathway suppresses growth of colon tumors *in vivo*. Nat Med 1999;5:810–6.
5. Yeh JJ, Routh ED, Rubinas T, et al. KRAS/BRAF mutation status and ERK1/2 activation as biomarkers for MEK1/2 inhibitor therapy in colorectal cancer. Mol Cancer Ther 2009;8:834–43.
6. Mirzoeva OK, Das D, Heiser LM, et al. Basal subtype and MAPK/ERK kinase (MEK)-phosphoinositide 3-kinase feedback signaling determine susceptibility of breast cancer cells to MEK inhibition. Cancer Res 2009;69:565–72.
7. Wee S, Jagani Z, Xiang KX, et al. PI3K pathway activation mediates resistance to MEK inhibitors in KRAS mutant cancers. Cancer Res 2009;69:4286–93.
8. Papadopoulos N, Kinzler KW, Vogelstein B. The role of companion diagnostics in the development and use of mutation-targeted cancer therapies. Nat Biotechnol 2006;24:985–95.
9. Harris L, Fritsche H, Mennel R, et al. American Society of Clinical Oncology 2007 update of recommendations for the use of tumor markers in breast cancer. J Clin Oncol 2007;25:5287–312.
10. Lievre A, Bachet JB, Le Corre D, et al. KRAS mutation status is predictive of response to cetuximab therapy in colorectal cancer. Cancer Res 2006;66:3992–5.
11. Stommel JM, Kimmelman AC, Ying H, et al. Coactivation of receptor tyrosine kinases affects the response of tumor cells to targeted therapies. Science 2007;318:287–90.
12. Ein-Dor L, Zuk O, Domany E. Thousands of samples are needed to generate a robust gene list for predicting outcome in cancer. Proc Natl Acad Sci U S A 2006;103:5923–8.
13. Paik S, Shak S, Tang G, et al. A multigene assay to predict recurrence of tamoxifen-treated, node-negative breast cancer. N Engl J Med 2004;351:2817–26.
14. van't Veer LJ, Dai H, van de Vijver MJ, et al. Gene expression profiling predicts clinical outcome of breast cancer. Nature 2002;415:530–6.
15. Bild AH, Yao G, Chang JT, et al. Oncogenic pathway signatures in human cancers as a guide to targeted therapies. Nature 2006;439:353–7.
16. Huang F, Reeves K, Han X, et al. Identification of candidate molecular markers predicting sensitivity in solid tumors to dasatinib: rationale for patient selection. Cancer Res 2007;67:2226–38.
17. Lee JK, Havaleshko DM, Cho H, et al. A strategy for predicting the chemosensitivity of human cancers and its application to drug discovery. Proc Natl Acad Sci U S A 2007;104:13086–91.
18. Pan KH, Lih CJ, Cohen SN. Effects of threshold choice on biological conclusions reached during analysis of gene expression by DNA microarrays. Proc Natl Acad Sci U S A 2005;102:8961–5.
19. Dupuy A, Simon RM. Critical review of published microarray studies for cancer outcome and guidelines on statistical analysis and reporting. J Natl Cancer Inst 2007;99:147–57.
20. Pavey S, Johansson P, Packer L, et al. Microarray expression profiling in melanoma reveals a BRAF mutation signature. Oncogene 2004;23:4060–7.
21. Bodmer LiuY. Analysis of P53 mutations and their expression in 56 colorectal cancer cell lines. Proc Natl Acad Sci U S A 2006;103: 976–81.
22. Finn RS, Dering J, Ginther C, et al. Dasatinib, an orally active small molecule inhibitor of both the src and abl kinases, selectively inhibits growth of basal-type/"triple-negative" breast cancer cell lines growing *in vitro*. Breast Cancer Res Treat 2007;105:319–26.
23. Xing F, Pratilas C, Persaud Y, et al. Genetic predictors of MEK dependence in V600 BRAF mutant melanoma. Proceedings of the 100th Annual Meeting of the American Association for Cancer Research, Denver, Colorado. 2009 Apr 18-22.
24. Pratilas CA, Taylor BS, Ye Q, et al. (V600E)BRAF is associated with disabled feedback inhibition of RAF-MEK signaling and elevated transcriptional output of the pathway. Proc Natl Acad Sci U S A 2009;106:4519–24.
25. Johansson P, Pavey S, Hayward N. Confirmation of a BRAF mutation-associated gene expression signature in melanoma. Pigment Cell Res 2007;20:216–21.
26. Rhodes DR, Yu J, Shanker K, et al. ONCOMINE: a cancer microarray database and integrated data-mining platform. Neoplasia 2004;6:1–6.
27. Adjei AA, Cohen RB, Franklin W, et al. Phase I pharmacokinetic and pharmacodynamic study of the oral, small-molecule mitogen-activated protein kinase kinase 1/2 inhibitor AZD6244 (ARRY-142886) in patients with advanced cancers. J Clin Oncol 2008;26:2139–46.
28. Creighton CJ, Hilger AM, Murthy S, Rae JM, Chinnaiyan AM, El Ashry D. Activation of mitogen-activated protein kinase in estrogen receptor α-positive breast cancer cells *in vitro* induces an *in vivo* molecular phenotype of estrogen receptor α-negative human breast tumors. Cancer Res 2006;66:3903–11.
29. Li C, Scott DA, Hatch E, Tian X, Mansour SL. Dusp6 (Mkp3) is a negative feedback regulator of FGF-stimulated ERK signaling during mouse development. Development 2007;134:167–76.
30. Brady SC, Coleman ML, Munro J, Feller SM, Morrice NA, Olson MF. Sprouty2 association with B-Raf is regulated by phosphorylation and kinase conformation. Cancer Res 2009;69:6773–81.
31. Oberst MD, Beberman SJ, Zhao L, Yin JJ, Ward Y, Kelly K. TDAG51 is an ERK signaling target that opposes ERK-mediated HME16C mammary epithelial cell transformation. BMC Cancer 2008;8:189.
32. Guo B, Sharrocks AD. Extracellular signal-regulated kinase mitogen-activated protein kinase signaling initiates a dynamic interplay between sumoylation and ubiquitination to regulate the activity of the transcriptional activator PEA3. Mol Cell Biol 2009;29:3204–18.

33. O'Hagan RC, Tozer RG, Symons M, McCormick F, Hassell JA. The activity of the Ets transcription factor PEA3 is regulated by two distinct MAPK cascades. Oncogene 1996;13:1323–33.

34. Eder K, Guan H, Sung HY, et al. Tribbles-2 is a novel regulator of inflammatory activation of monocytes. Int Immunol 2008;20: 1543–50.

35. Saegusa J, Hsu DK, Liu W, et al. Galectin-3 protects keratinocytes from UVB-induced apoptosis by enhancing AKT activation and suppressing ERK activation. J Invest Dermatol 2008;128:2403–11.

36. Baldassarre G, Croce CM, Vecchione A. Take your "M" time. Cell Cycle 2007;6:2087–90.

37. Onken MD, Worley LA, Harbour JW. A metastasis modifier locus on human chromosome 8p in uveal melanoma identified by integrative genomic analysis. Clin Cancer Res 2008;14:3737–45.

38. Cordenonsi M, Montagner M, Adorno M, et al. Integration of TGF-β and Ras/MAPK signaling through p53 phosphorylation. Science 2007;315:840–3.

39. Kreeger PK, Mandhana R, Alford SK, Haigis KM, Lauffenburger DA. RAS mutations affect tumor necrosis factor-induced apoptosis in colon carcinoma cells via ERK-modulatory negative and positive feedback circuits along with non-ERK pathway effects. Cancer Res 2009;69:8191–9.

40. Carlson JA, Linette GP, Aplin A, Ng B, Slominski A. Melanocyte receptors: clinical implications and therapeutic relevance. Dermatol Clin 2007;25:541–ix.

41. Ancrile B, Lim KH, Counter CM. Oncogenic Ras-induced secretion of IL6 is required for tumorigenesis. Genes Dev 2007;21:1714–9.

42. Fenton JI, Lavigne JA, Perkins SN, et al. Microarray analysis reveals that leptin induces autocrine/paracrine cascades to promote survival and proliferation of colon epithelial cells in an Apc genotype-dependent fashion. Mol Carcinog 2008;47:9–21.

43. Zhang H, Kim JK, Edwards CA, Xu Z, Taichman R, Wang CY. Clusterin inhibits apoptosis by interacting with activated Bax. Nat Cell Biol 2005;7:909–15.

44. Liu J, Hamrouni A, Wolowiec D, et al. Plasma cells from multiple myeloma patients express B7-H1 (PD-L1) and increase expression after stimulation with IFN-γ and TLR ligands via a MyD88-, TRAF6-, and MEK-dependent pathway. Blood 2007;110:296–304.

45. Legrier ME, Yang CP, Yan HG, et al. Targeting protein translation in human non small cell lung cancer via combined MEK and mammalian target of rapamycin suppression. Cancer Res 2007;67:11300–8.

46. Pratilas CA, Hanrahan AJ, Halilovic E, et al. Genetic predictors of MEK dependence in non-small cell lung cancer. Cancer Res 2008; 68:9375–83.

47. Hodgson DR, Whittaker RD, Herath A, Amakye D, Clack G. Biomarkers in oncology drug development. Mol Oncol 2009;3:24–32.

Cancer Research

The Journal of Cancer Research (1916–1930) | The American Journal of Cancer (1931–1940)

AACR American Association for Cancer Research

Transcriptional Pathway Signatures Predict MEK Addiction and Response to Selumetinib (AZD6244)

Jonathan R. Dry, Sandra Pavey, Christine A. Pratilas, et al.

Updated version	Access the most recent version of this article at: doi:10.1158/0008-5472.CAN-09-1577
Supplementary Material	Access the most recent supplemental material at: http://cancerres.aacrjournals.org/content/suppl/2010/03/08/0008-5472.CAN-09-1577.DC1

Cited articles	This article cites 46 articles, 26 of which you can access for free at: http://cancerres.aacrjournals.org/content/70/6/2264.full#ref-list-1
Citing articles	This article has been cited by 60 HighWire-hosted articles. Access the articles at: http://cancerres.aacrjournals.org/content/70/6/2264.full#related-urls

E-mail alerts	Sign up to receive free email-alerts related to this article or journal.
Reprints and Subscriptions	To order reprints of this article or to subscribe to the journal, contact the AACR Publications Department at pubs@aacr.org.
Permissions	To request permission to re-use all or part of this article, use this link http://cancerres.aacrjournals.org/content/70/6/2264. Click on "Request Permissions" which will take you to the Copyright Clearance Center's (CCC) Rightslink site.